

Physical Characteristics of Coal Reservoirs and CBM Favorable Area Prediction in the Huaibei Coalfield, Northern China

Xuejiao Zhou, Bo Hu, Qian He, Xiangqin Huang, and Haihai Hou*

Cite This: *ACS Omega* 2024, 9, 12158–12174

Read Online

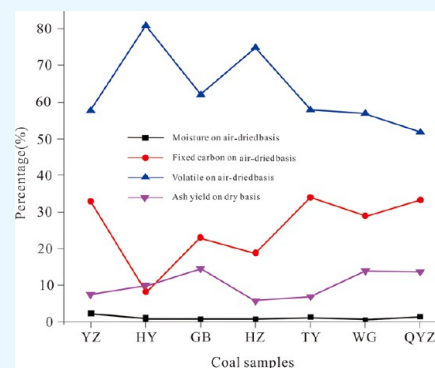
ACCESS |

Metrics & More

Article Recommendations

ABSTRACT: To quantitatively characterize middle-high-ranked coal reservoirs, the physical characteristics of seven coal samples from the Huaibei Coalfield in northern China were investigated in detail based on experiments including proximate analysis, coal petrology, low-temperature nitrogen adsorption (LTNA), mercury intrusion porosimetry (MIP), nuclear magnetic resonance (NMR), and methane isothermal adsorption. The results show that coal maceral in the Huaibei Coalfield is dominated by vitrinite, with a large change in the maximum vitrinite reflectance ranging from 0.7 to 2.5%. The various coal metamorphisms can be attributed to the combined influence of magmatic activities of the Tanlu and Taihang Mountains during the Yanshanian. The coal quality can be characterized by medium-high ash yield, low to very low sulfur content, low phosphorus, and medium-high calorific value. From low-ranked coals to medium-ranked coals, the volume of adsorption and seepage pores decreases but the fracture volume increases due to the stronger dehydration and coal matrix shrinkages.

From medium-ranked coals to high-ranked coals, adsorption pores have a significant advantage, suggesting a stronger CH₄ adsorption capacity. There is a positive correlation among the fixed carbon content, coal rank, and Langmuir volume, which can be attributed to the transformation of coal chemical composition and structure by coal metamorphism. The deep Xiaoxi in the Suixian coal mining area, deep Nanping, deep Taoyuan–Qinan, deep Pengqiao, northern Zhuxianzhuang in the Suxian coal mining area, deep Renlou–Zhaoji, and Xutuan deep in the Linhuan mining area are predicted to be favorable areas for CBM exploration in the Huaibei Coalfield.



1. INTRODUCTION

In China, the coalbed methane (CBM) production of ground wells has increased gradually in recent years, with a total production of 83×10^8 m³ in 2021.¹ However, the majority of the CBM production depends on the middle-high-ranked coal regions of the eastern Ordos Basin and the southern Qinshui Basin.^{2–4} Since 1994, various companies both domestic and international have been engaged in CBM exploitation in the Huaibei Coalfield (northern China),^{5,6} with the maximum daily production reaching 0.5×10^4 m³ from a single vertical well. There are abundant CBM resources in the Huaibei Coalfield; however, the efficiency is not very desirable between CBM exploration input and output, which can be attributed to the heterogeneity of the physical properties of coal reservoirs to some degree.

Unlike conventional sandstone and carbonate rocks, coal reservoirs have special characteristics of a double porosity (pore-fracture) structure, which affects a series of CBM exploitation processes including adsorption, desorption, diffusion, and seepage.^{7,8} Compared with the influence of pores on CBM sorption/permeability, the initial classification was proposed by Hodot,⁹ where the pore type can be classified into adsorption pores of pore size ranging from 0 to 100 nm and seepage pores of pore size larger than 100 nm.^{10,11} The adsorption pores mainly

affect the physical sorption and desorption of coalbed methane; thus, they are closely related to the methane adsorption ability and desorption velocity, which are usually tested by the low-temperature nitrogen adsorption (LTNA) experiment.^{12,13} The seepage ability mainly depends on the development of seepage pores, and the distribution of the seepage pores in the coal reservoir can be determined by the mercury intrusion porosimetry (MIP) experiment.¹⁴ However, the pore/fracture system of the primary coal structure can be destroyed more or less through both experiments mentioned above. Therefore, new nondestructive detection technologies including nuclear magnetic resonance (NMR) and X-ray computed topography (CT) have been used to characterize the pore-fracture development of the coal reservoir in recent years.^{15,16}

For the coalbed methane of the Carboniferous–Permian strata in the Huaibei Coalfield, previous investigations had

Received: January 2, 2024
Revised: February 1, 2024
Accepted: February 9, 2024
Published: February 29, 2024



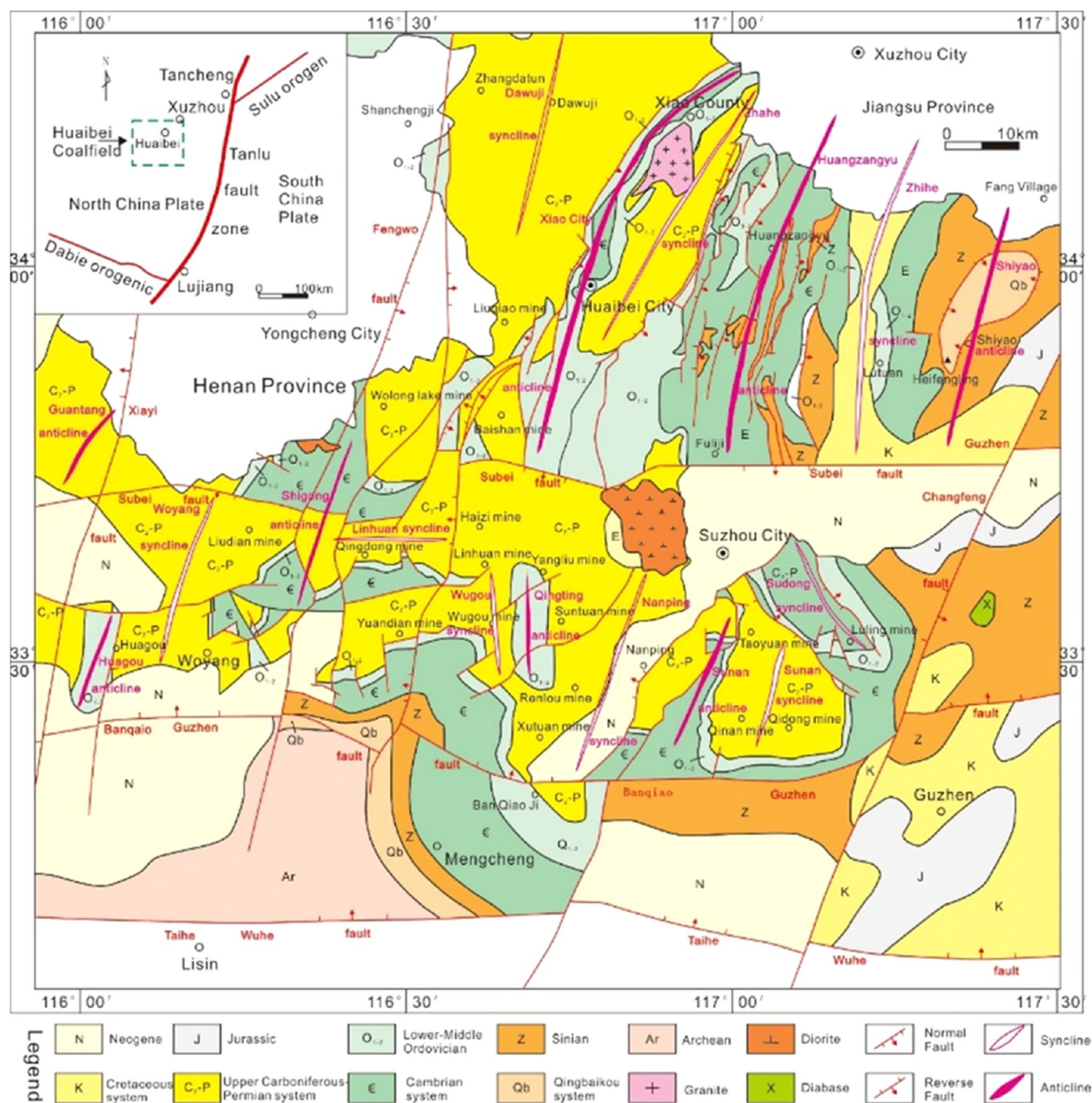


Figure 1. Map showing the structure outline of the Huaibei Coalfield in northern China.

mainly focused on the CBM occurrence conditions, enrichment conditions, and their influencing factors.^{17,18} Based on the coal sampling regionally and a series of experiments including proximate analysis, vitrinite reflectance determination, maceral micro-observation, LTNA, MIP, NMR, and methane adsorption, the pore/fracture characteristics of coal reservoirs and their evolution rules along with the factors influencing methane adsorption ability were analyzed. Then, the distributions of coal reservoirs were evaluated and potential areas for CBM exploration and development were proposed. Finally, several CBM exploration wells can be implemented based on reservoir optimization results, and a comparative analysis of the reservoir parameters obtained from the wells can be performed in the future.

2. GEOLOGICAL SETTINGS

The Huaibei Coalfield is located in the southeast margin of the North China Plate, bordering the Yangtze Plate in the east and the Bengbu Uplift in the south.¹⁹ The geological structure in this area is influenced by the EW-trending structure and the Tanlu fault, resulting in an EW-trending and NE-trending structure framework in the Huaibei Coalfield (Figure 1). The Carboniferous–Permian is the main coal-bearing strata in this area, which consists of the Shanxi Formation, the lower Shihezi Formation, and the upper Shihezi Formation.²⁰ In the early Shanxi Formation, a regional regression from the north to the south occurred, and a barrier lagoon sedimentary system was developed, forming several recoverable coal seams in the lower part of the Shanxi Formation with onshore delta deposits. Then,

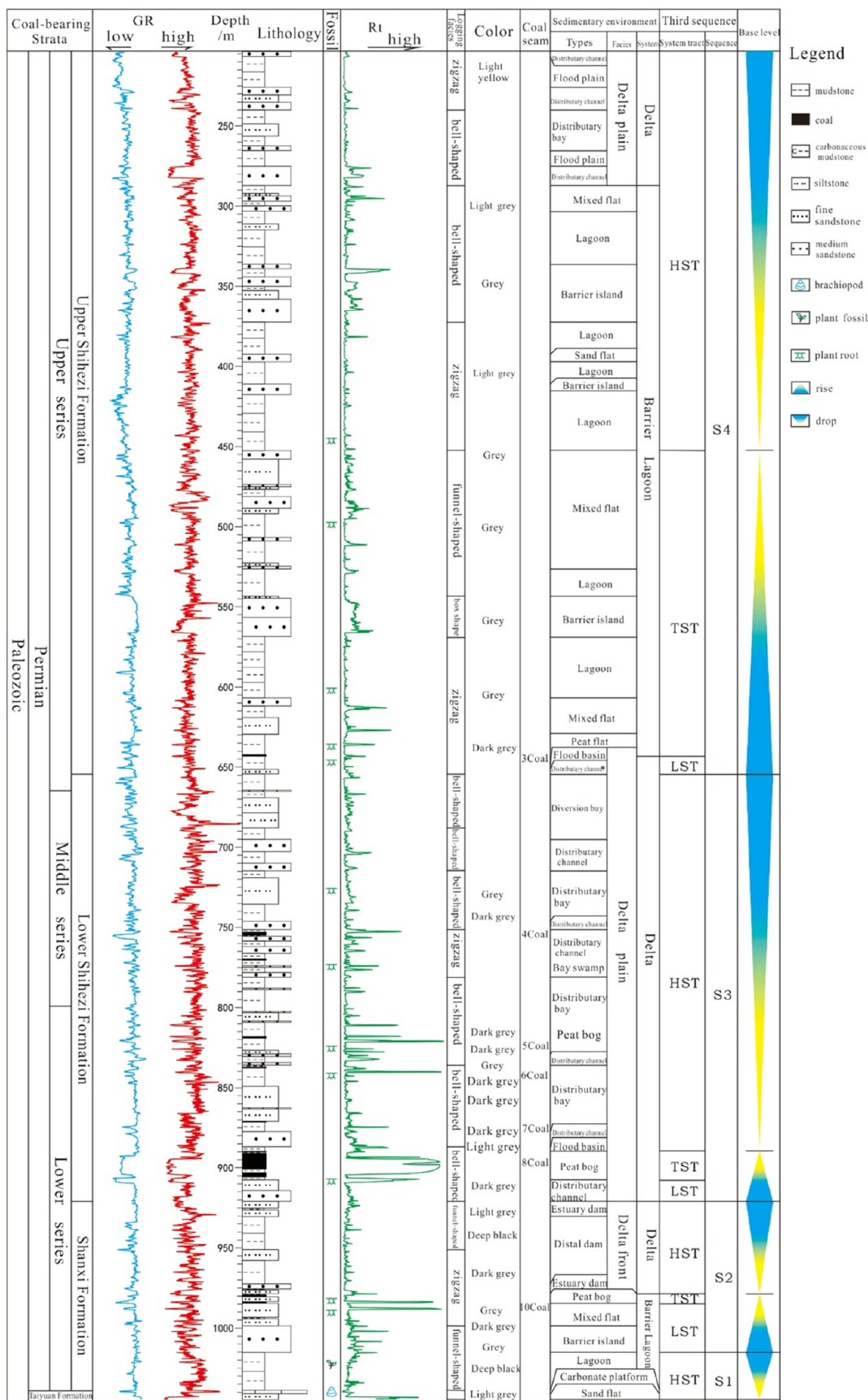


Figure 2. Sedimentary column diagram of well L24 in the Luling coal mine, Huaibei Coalfield.

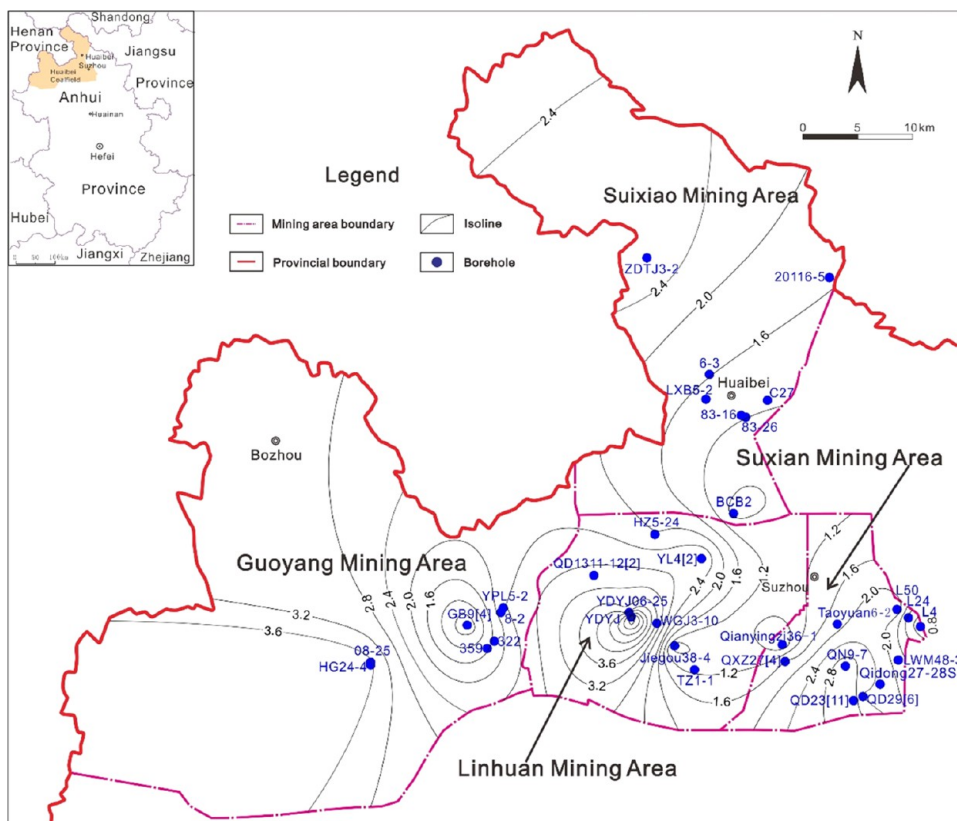


Figure 3. Thickness contour map of No.10 coal in the Huaibei Coalfield.

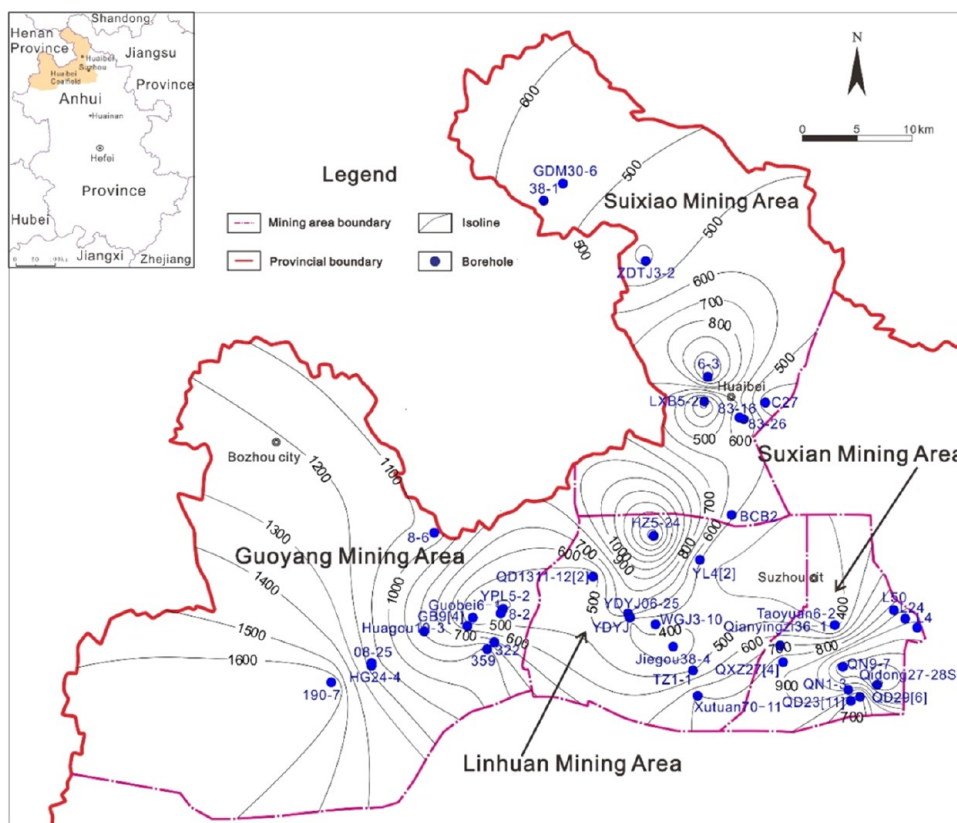


Figure 4. Contour map of coal depth No.10 coals in the Huaibei Coalfield.

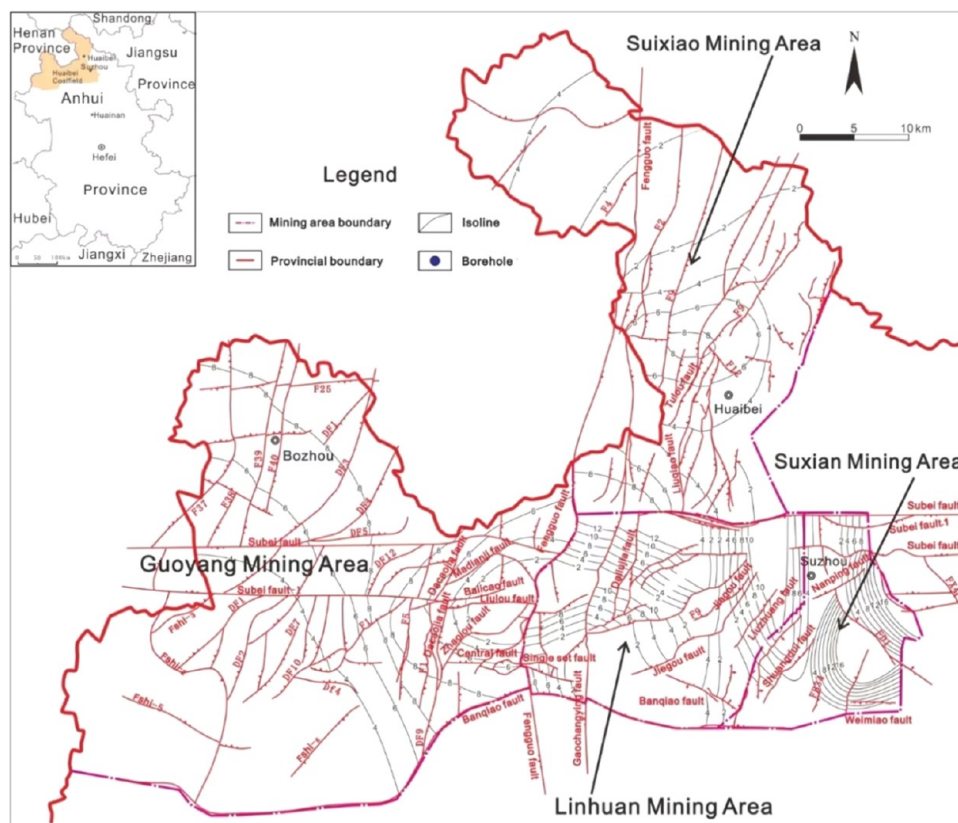


Figure 5. Contour map of the gas content of No.10 coals in the Huaibei Coalfield.

as the seawater continued to retreat to the south, the delta plain was formed widely with a large number of recoverable coal seams in the lower Shihezi Formation (Figure 2). At the end of the early Permian, the delta in this area experienced many turbulent events, leading to the formation of a large number of intermittent, unrecoverable coal seams. Generally, there are abundant coal and CBM resources in the Huaibei Coalfield, including Suixiao, Guoyang, Linhuan, and Suxian coal minings (Figure 1).

Nos. 7–2 and 8–2 coal seams of the Lower Shihezi Formation and No. 10 coal seam of the Shanxi Formation in Huaibei Coalfield are the main objects for CBM exploration.⁸ Taking No. 10 coal seam as an example, the variations in coal thickness, burial, and gas contents were introduced in detail. The coal thickness of the No. 10 seam is between 0.35 and 6.3 m, with an average of 1.4 m, with a tendency to be thicker in the south and thinner in the north. It should be noted that thin belts are found in the Suixiao and Linhuan mining areas in the NE direction and the Guoyang mining area in the NW direction, which may be caused by the river scour surface.²¹ In the Linhuan coal mining, coal seams with more than 6 m thickness are found close to the Yuanzhuang region, and seams that are more than 3 m thick in the Qixian coal mine are found close to the Qinan region (Figure 3).

The coal burial depth in the Guoyang coal mining exhibits an increasing trend from the east to the west, with the maximum burial depth exceeding 1600 m.⁸ The area with burial depth less than 500 m only appears in a small region in the east of Guobei. In the Suixiao coal mining, the largest burial depth is found in the middle part, which becomes shallow toward the north and the south, with the deepest depth exceeding 1100 m (Figure 4).

The gas content of the Huaibei Coalfield generally has an obvious positive correlation with burial depth in the middle and shallow parts. For the gas content of the No. 10 coal seam, the distribution is characterized by higher values in the east and south and lower values in the west and north, with the highest being in the southeast (Figure 5). The gas contents and methane concentrations in the Suxian, Linhuan, Suixiao, and Guoyang coal minings are 6–24 m³/t and 79–99%, 6–16 m³/t and 75–91%, 2–12 m³/t and 60–79%, and 2–8 m³/t and 40–80%, respectively.

3. SAMPLING AND EXPERIMENTAL METHODS

Based on the distribution of coal mines in the Huaibei Coalfield, seven coal samples were collected from seven coal mines, including Yuanzhuang, Hengyuan, Guobei, Haizi, Wugou, Taoyuan, and Qianyingzi coal mines. In order to characterize the physical features of coal reservoirs in detail, basic tests and advanced tests were performed in this study. Specifically, the basic tests consist of proximate analysis, vitrinite reflectance, coal maceral identification, and coal macrolithotype description. The advanced tests consist of low-temperature nitrogen adsorption, high-pressure Hg injection, nuclear magnetic resonance, and methane isothermal adsorption. The coal proximate analysis parameters, including the moisture content, ash yield, volatile content, and fixed carbon, were obtained based on the Chinese Standard GB/T 212–2008. Vitrinite reflectance ($R_{o,max}$) measurements and maceral analyses (500 points) were performed by oil immersion in reflected optical light using a Leitz MPV-3 photometer microscope, in accordance with Chinese Standards GB/T 6948–1998 and GB/T 8899–1998, respectively. Based on the macrolithotype description, the samples were divided into four types, including bright,

Table 1. Proximate Analysis and Vitrinite Reflectance Results of the Huaibei Coalfield

sampling site	proximate analysis/%						$R_{o,max}/\%$	
	M_{ad}	A_{ad}	V_{ad}	FC_{ad}	A_d	V_d	range	average
Yuanzhuang mine	2.35	7.25	32.85	57.55	7.42	33.64	0.52–0.68	0.59
Hengyuan mine	0.99	9.89	8.18	80.94	9.99	8.26	1.96–2.36	2.12
Guobei mine	0.64	14.4	22.94	62.02	14.49	23.09	1.31–1.54	1.4
Haizi mine	0.6	5.76	18.71	74.93	5.79	18.82	1.41–1.63	1.5
Taoyuan mine	1.28	6.8	33.94	57.98	6.89	34.38	0.52–0.71	0.6
Wugou mine	0.54	13.81	28.78	56.87	13.88	28.94	0.92–1.27	1.08
Qianyingzi mine	1.4	13.42	33.24	51.94	13.61	33.71	0.68–0.87	0.76

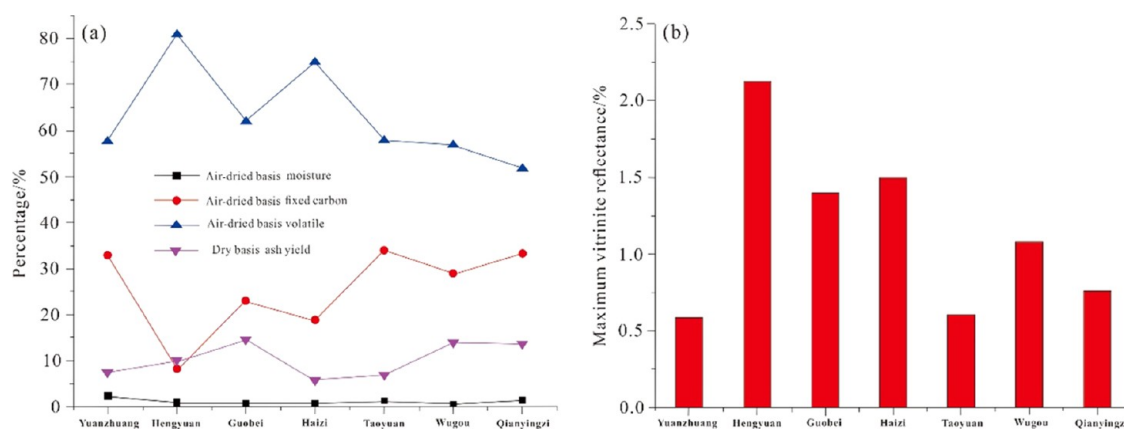


Figure 6. Proximate analysis and maximum vitrinite reflectance of coal samples in the Huaibei Coalfield.

semibright, semidull, and dull coals, with bright compositions of >80, 50–80, 20–50, and <20%, respectively. Nitrogen adsorption is used to obtain the specific surface area, pore volume, and pore structure distribution of adsorption pores, which was tested by the NOVA2000e specific surface area and aperture analyzer. High-pressure Hg injection was conducted following the national petroleum industry standard SY/T 5346–2005 on a Quantachrome PoreMaster 33 high-pressure porosimeter. The nuclear magnetic resonance measurements were conducted using an NMR analyzer (MicroMR12–025 V) with a resonant frequency of 11.854 MHz and a magnet temperature of 35.00 ± 0.02 °C. Methane adsorption experiments were performed under isothermal conditions on moisture-equilibrated samples using an IS-100 high-pressure isothermal adsorption apparatus at 30 °C and a maximum equilibrium pressure of 10 MPa.

4. RESULTS AND DISCUSSION

4.1. Proximate Analysis. According to the regional testing data, the coals in the Huaibei Coalfield are characterized by medium-high ash yield, low to very low sulfur content, low phosphorus, and medium-high calorific values. For the various coal seams in the Huaibei Coalfield, the ash yield is between 6.01 and 43.97% with an average of 22.03% and the sulfur content is between 6.53 and 47.09% with an average of 11.84%. The volatile matter of Huaibei coals varies from 6.53 to 47.09%, which has a negative correlation with burial depth. Based on the testing data in this study, the moisture content on an air-dried basis of the coal samples ranges from 0.54 to 2.35%, with an average of 1.11% (Table 1), which is negatively correlated with the coalification degree. The water content of Yuanzhuang coal, with the lowest metamorphism, exhibits the highest value at 2.35%. The water contents of Hengyuan, Guobei, Haizi, and Wugou coals with the $R_{o,max}$ exceeding 1% is less than 1%,

whereas the water content of Yuanzhuang, Taoyuan, and Qianyingzi coals with $R_{o,max}$ less than 1% is between 1.28 and 2.35%.

The ash yield on an air-dried basis of coal samples in the Huaibei Coalfield is 5.76–14.4%, with an average of 10.19%, placing them within the category of ultralow-ash to low-ash coal. The ash yield of Yuanzhuang mine, Hengyuan mine, Haizi mine, and Taoyuan mine is low, with their values less than 8%, placing them within the category of ultralow-ash coal. The Guobei, Wugou, and Qianyingzi mines have high ash yields, with their values larger than 13%, placing them within the category of low-ash coal. The volatile on an air-dried basis of coal samples in the Huaibei Coalfield is between 8.18 and 33.94%, with an average of 25.52%, which has a good negative correlation with the maximum vitrinite reflectance. Generally, coalification is a dehydration process;^{22,23} thus, the coal sample from the Hengyuan mine with the highest degree of metamorphism has the lowest volatile yield of 8.18%. The coal samples from Yuanzhuang, Taoyuan, and Qianyingzi mines with low metamorphism have higher volatile yields, with more than 30% volatiles on an air-dried basis, placing them within the category of medium- to high-volatile coals (Figure 6a).

The fixed carbon content of coal samples in the Huaibei Coalfield is 51.94–80.94%, with an average of 63.18%, which has a strong correlation with the metamorphism degree. The fixed carbon content of Hengyuan coal is the highest (80.94%), with the highest metamorphism degree. The fixed carbon content of Yuanzhuang, Taoyuan, Wugou, and Qianyingzi coals is relatively low with a lower metamorphism degree, all of which are less than 60%.

4.2. Vitrinite Reflectance Determination and its Analysis. Two different belts of coal species are found in the Huaibei Coalfield. One belt is situated in the south of Linhuan–Suzhou, which is characterized by gas coals and fat coals in most



Figure 7. Macroscopic characteristics of coal samples in the Huaibei Coalfield (1, Yuanzhuang; 2, Hengyuan; 3, Guobei; 4, Haizi; 5, Wugou; 6, Taoyuan; 7, Qianyingzi).

areas and coking coals and anthracites in some areas. Another belt is situated in the north of Linhuan–Suzhou, which is characterized by lean coal, anthracite, and natural coke.⁸ The maximum vitrinite reflectance in the Huaibei Coalfield is between 0.7 and 2.5%, with the most likely range being from 0.75 to 1.1%. The maximum vitrinite reflectance of the coal samples varies from 0.59 to 2.12%, with an average of 1.15%, placing them within the category of long flame coals and lean

coals (Figure 6b), and it has a good positive correlation with coal burial depth.²⁴ Additionally, the distribution of coal metamorphism degree is also closely related to magmatic intrusion in the Huaibei Coalfield,²⁵ with the vitrinite reflectance of coals near magmatic intrusion belts usually being higher compared with other regions. Generally, there are various coal metamorphism in the Huaibei Coalfield, which is attributed to the

Table 2. Low-Temperature Nitrogen Testing Results of Coal Samples from the Huaibei Coalfield^a

sampling site	SSA/m ² /g	MPPZ/nm	TPV/10 ⁻³ cm ³ /g	volume percentage/%			area percentage/%		
				micropore	TP	mesopore	micropore	TP	mesopore
Yuanzhuang mine	0.561	4.016	1.643	33.16	43.3	23.54	78.21	20.01	1.78
Hengyuan mine	0.254	4.026	0.766	37.39	38.44	24.17	82	16.69	1.31
Wobei mine	0.48	4.028	1.023	45.88	38.79	15.33	84.27	14.88	0.85
Haizi mine	0.393	3.608	0.728	51.54	34.39	14.07	86.72	12.8	0.48
Taoyuan mine	0.43	4.013	1.007	46.45	46.94	6.61	83.07	16.61	0.32
Wugou mine	0.446	3.226	1.159	38.32	53.78	7.9	76.75	22.68	0.57
Qianyingzi mine	0.697	3.07	1.712	40.65	39.09	20.26	82.58	16.18	1.24

^aSSA, specific surface area; MPPZ, most probable pore size; TPV, total pore volume; TP, transitional pore.

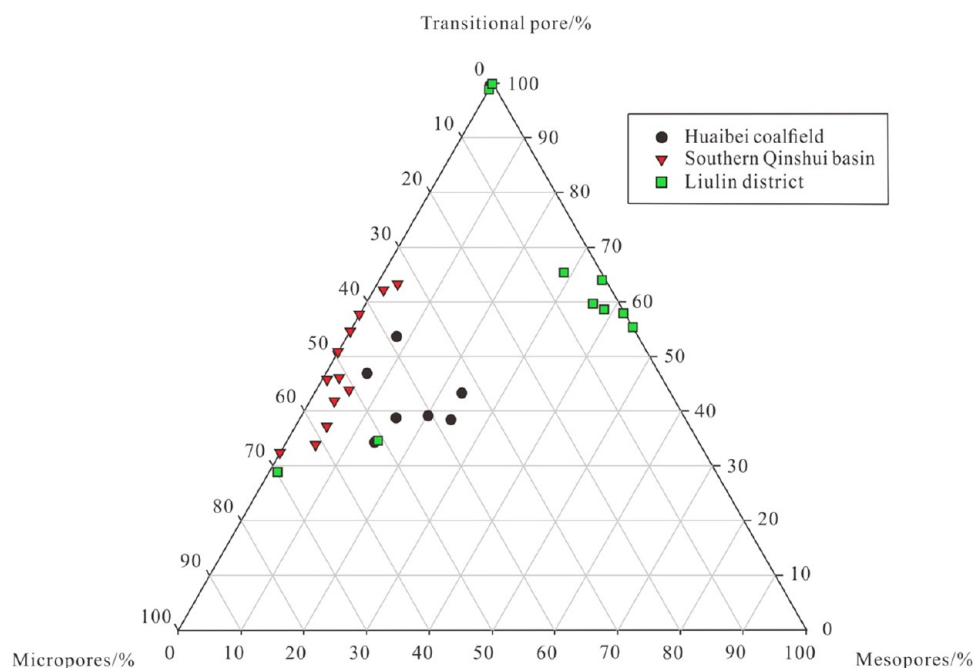


Figure 8. Pore distribution comparison from the Huaibei Coalfield, southern Qinshui Basin, and Hedong district.

combined influence of magmatic activities of Tanlu, Taihang Mountain, and Shanxi rift zones in the Yanshanian.²⁶

4.3. Coal Macrolithotype and Coal Maceral Analysis.

The coal macro-features of the coal samples can be described as follows. The macrolithotype of the Yuanzhuang mine is semidull and semibright with a cataclastic structure and conchoidal fracture. The macrolithotype of Hengyuan mine is bright coal with a cataclastic and bedded structure. The macrolithotype of Guobei mine is semidull and semibright with a granular structure and well-developed calcite vein filled in the fractures. The macrolithotype of Haizi and Wugou mines is semidull and semibright with a cataclastic and bedded-like structure. The macrolithotypes of Taoyuan and Qianyingzi mines are semibright with a cataclastic and bedded structure and an uneven fracture (Figure 7). Based on previous investigations, coal macrolithotypes can be largely determined by the depositional environment (especially coal facies), with bright coals in forest swamp facies, semibright and semidull coals in active water swamp facies, and dull coals in dry swamp facies.^{27,28} Therefore, the water level in the Hengyuan coal mine would be the deepest, followed by Taoyuan, Qianyingzi, Guobei, Haizi, Wugou, and Yuanzhuang coal mines.

In terms of coal macerals, vitrinite is the predominant component in Huaibei coals, ranging from 58.5 to 87.1%, with an average of 73.4%. Inertinite is the secondary component,

ranging from 10.98 to 32.39%, with an average of 21.75%, and exinite is the minimum, ranging from 0.38 to 11.94%, with an average of 4.86%. Except for the Taoyuan coal mine, the exinite contents of other coal mines are not more than 10%. This indicates that repeated wildfires in the Carbonate–Permian strata in the Huaibei Coalfield did not occur.^{29,30}

4.4. Coal Reservoir Physical Characteristics. **4.4.1. Low-Temperature N₂ Adsorption.** The total pore volume of the coal samples varies from 0.728 to 1.712 × 10⁻³ cm³/g with an average of 1.148 × 10⁻³ cm³/g, which decreases with increasing coal rank (Table 2). Therefore, the total pore volumes of Yuanzhuang and Qianyingzi coals are higher than 1.5 × 10⁻³ cm³/g due to the lower coalification degree. The percentage of micropore and transitional pore volumes is much larger, with a similar contribution ranging from 33.16 to 51.54% (average, 41.91%) and 34.39 to 53.78% (average, 42.10%), respectively. Compared with the southern Qinshui Basin and Liulin district in the Hedong Coalfield, the micropore content of Huaibei coals is lower than that in the southern Qinshui Basin and the mesopore content of Huaibei coals is lower than that in Liulin district (Figure 8).

The specific surface area of Huaibei coals is between 0.254 and 0.697 m²/g, with an average of 0.466 m²/g, accounting for 81.94% of the micropores, 17.12% of the transitional pores, and 0.94% of the mesopores. Based on N₂ adsorption–desorption

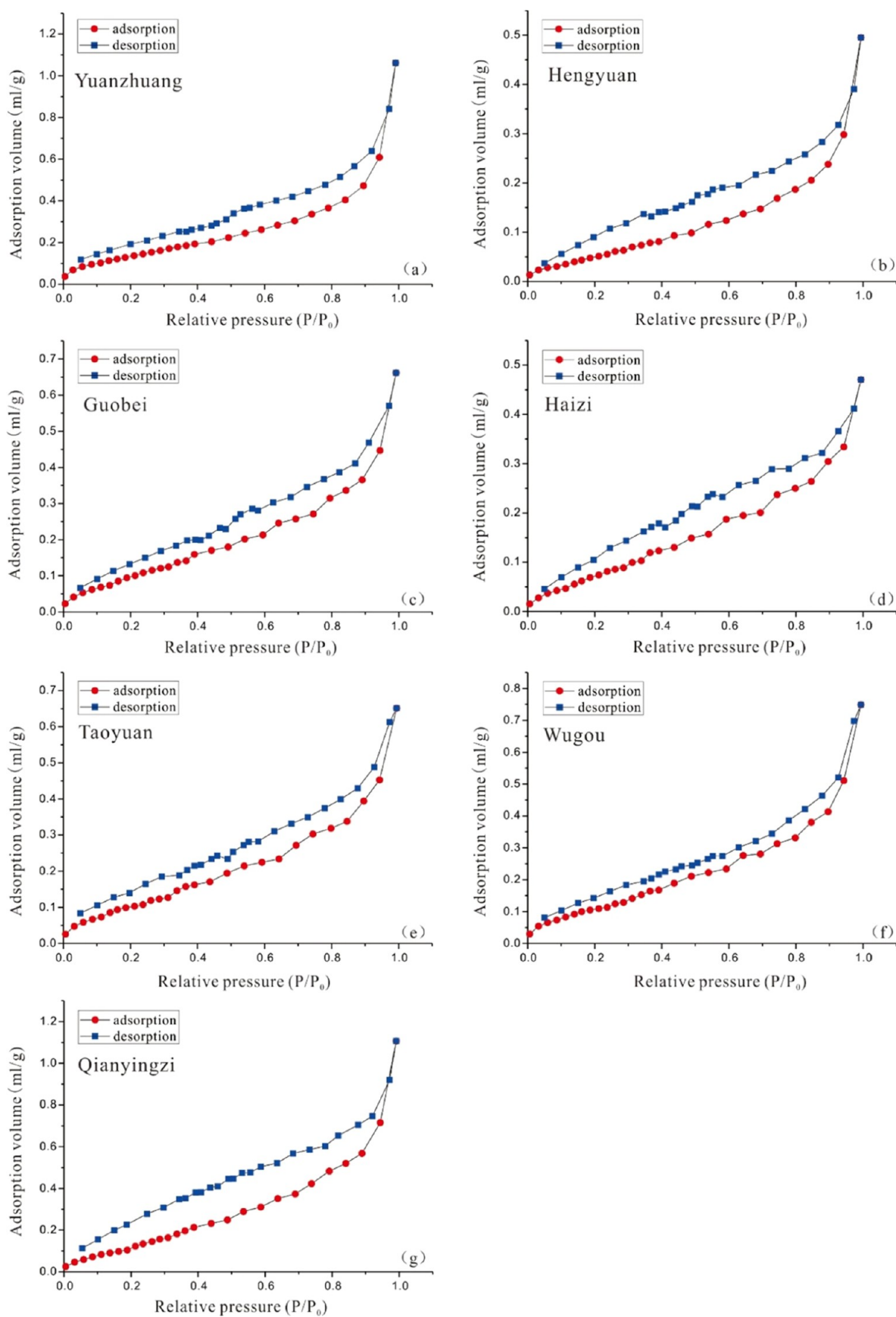


Figure 9. Characteristics of low-temperature nitrogen adsorption–desorption curves of Huaibei coals.

Table 3. Parameters of Mercury Injection, Porosity, and Permeability of Huaibei Coals^a

sampling site	displacement pressure (MPa)	saturated median pressure (MPa)	median pore radius (μm)	maximum mercury saturation (%)	mean pore radius (μm)	mercury drainage efficiency (%)	pore distribution(%)				
							macropore	mesopore	transitional pore	porosity (%)	permeability (mD)
Yuanzhuang mine	2.07	45.79	0.016	71.919	0.066	58.18	2.91	25.63	71.47	2.664	0.034
Hengyuan mine	0.14	47.938	0.015	67.32	0.839	69.07	33.32	13.80	52.87	1.532	0.002
Wugou mine	5	-	-	29.874	0.016	83.18	2.88	43.46	53.66	4.842	0.386

^aNote: ‘-’ indicates that the maximum mercury saturation does not reach 50%, and the corresponding parameters are not measured.

curves, four different pore types can be distinguished (Figure 9). The first type is represented by Taoyuan and Wugou coals with small adsorption loops, indicating that the pore type is dominated by nonparallel plate pores. The second type is represented by Hengyuan and Haizi coals with large adsorption loops, indicating that the pore type is dominated by parallel plate holes. The third type is represented by Qianyingzi coal with unclosed adsorption loops, indicating that the pore type contains more parallel plate holes with open mouths. The fourth type is represented by Yuanzhuang and Guobei coals with a sharp drop at the relative pressure (P/P_0) of 0.5, suggesting that the pore type is dominated by parallel plate holes and ink bottle holes. Due to the presence of ink bottle holes, the fourth pore type is the most complicated compared with the other pore types, which is advantageous for gas adsorption but disadvantageous for gas diffusion and seepage.³¹

4.4.2. Mercury Intrusion Porosimetry. The median saturation pressure and pore radius of Yuanzhuang and Hengyuan coals are similar to lower displacement pressures and higher maximum mercury saturation and efficiency of mercury drainage (Table 3). Although the pore radius of Hengyuan coal is larger, the pore shape is of a semiclosed type and the porosity is low, with poor connectivity and permeability. In terms of Yuanzhuang coal, the proportion of mesopores and transitional pores is large, and the pore types are open, with good connectivity and permeability. Wugou coal has a low displacement pressure, maximum mercury saturation, and average pore radius. The pore shape is mainly of a semiclosed type, but the proportion of mesopores and transitional pores, the mercury removal efficiency, and the porosity are high, with good connectivity and high permeability.

Based on a comprehensive analysis of mercury injection, low-temperature nitrogen adsorption, and pore permeability testing, Yuanzhuang coal has a large specific surface area and good pore connectivity, which is favorable to the adsorption, desorption, and diffusion of coalbed methane. However, due to the small proportion of porosity and large pores, it is unfavorable to gas seepage (Figure 10). The lower specific surface area and micropores in Hengyuan coal are not conducive to gas adsorption. The existence of semiclosed pores and the low content of medium pores may affect the effective diffusion of gas, and the lower porosity is not conducive to gas seepage (Figure 11). Both the specific surface area and porosity of Wugou coal are large, which are favorable for gas adsorption and seepage, but the existence of one-end-closed pore may affect the effective gas diffusion (Figure 12).

4.4.3. Nuclear Magnetic Resonance. Based on previous investigations, the T_2 relaxation time of adsorption pores ranges from 0.5 to 2.5 ms, with seepage pores ranging from 20 to 50 ms, and fractures being higher than 100 ms.³² Nuclear magnetic

resonance (NMR) was performed on five samples, including Yuanzhuang, Hengyuan, Guobei, Haizi, and Wugou mines, and the results are shown in Table 4 and Figure 13. The T_2 relaxation time distributions of various samples are different due to the difference in the pore structure. A triple peak pattern of the T_2 relaxation time can be identified from Wugou and Haizi coals, which indicates that adsorption pores, seepage pores, and fractures are well-developed. The adsorption pores are well-developed and the development of seepage pores is not obvious, suggesting that the connectivity between adsorption and seepage pores is poor. Generally, the low-ranked coals from Yuanzhuang mine have well-developed adsorption and desorption pores, whereas adsorption pores are well-developed but seepage pores are not developed in high-ranked coals from Hengyuan mine. In terms of medium-ranked coals from Wugou, Haizi, and Guobei mines, there are typically three peaks with high permeability and better pore connectivity (Table 4). From low-ranked coals to medium-ranked coals, the volume of adsorption and seepage pores decreases and the fracture volume increases due to the stronger dehydration and coal matrix shrinkages.^{33,34} From medium-ranked coals to high-ranked coals, adsorption pores have a significant advantage, suggesting a higher CH_4 adsorption capacity.^{34,35}

4.4.4. CH_4 Adsorption Characteristics. A CH_4 isothermal adsorption experiment was performed on four coal samples from Yuanzhuang, Hengyuan, Guobei, and Haizi mines (Figure 14). There is a good positive correlation between the coalification degree and the CH_4 adsorption capacity (Figure 15a), which was supported by previous investigations.^{36,37} Among the many factors affecting the coal adsorption capacity, it is generally believed that coal rank is one of the most important factors. Yee et al.³⁸ found that there is a U-shaped relation between the Langmuir volume and coal rank in terms of coals on a dry basis. Su et al.³⁹ discussed the relationship between the adsorption capacity of coal and coal rank under equilibrium water conditions and found that the change rule of the adsorption capacity with coal rank can be divided into four stages, which correspond to the four coalification jumps attributed to the effects of the pores, structure, and physical and chemical properties caused by coalification. Zhao et al.⁴⁰ pointed out that the coal chemical composition and structure can be changed by coalification, resulting in the continuous reduction of the hydrophilic chemical composition in coal and increasing the methane adsorption capacity.

There is a positive correlation between the fixed carbon content and the Langmuir volume (Figure 15b), suggesting that coals with a high fixed carbon content usually have a high CH_4 adsorption capacity.³⁹ Increasing carbon content is a typical feature of the coal metamorphic process, reaching almost complete carbonization with an aromatized structure.⁴¹ Indeed,

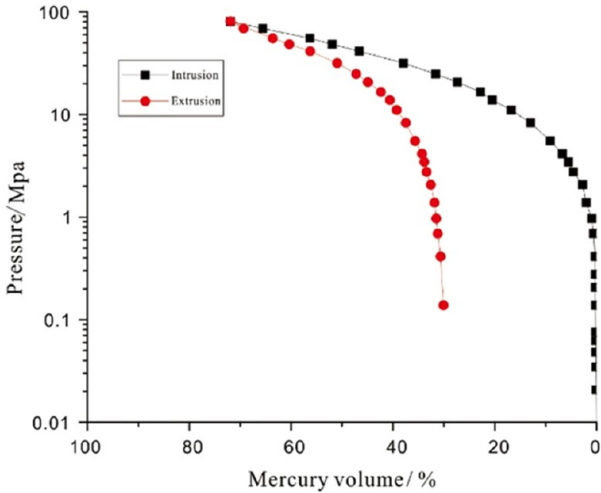
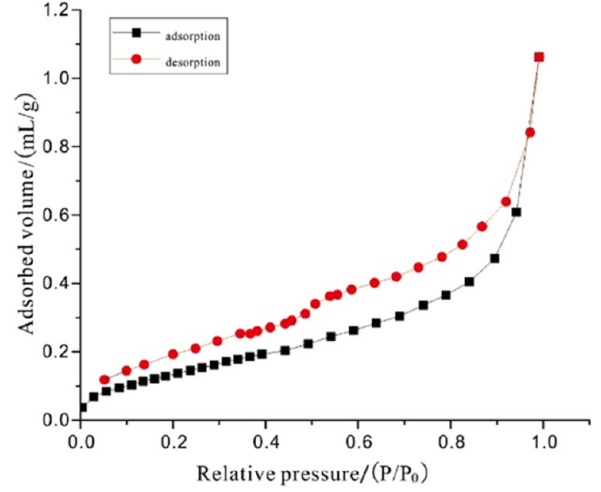
Pore structure testing method		Pore structure parameter		Value	Evalua-tion	General analysis
 <p>Mercury injection/extrusion curves of Yuanzhuang coal</p>	Pore distribution (%)	Macropore	2.91	A better connectivity, it is favorable to CBM diffusion, unfavorable to seepage and CBM production. to seepage.		
		Mesopore	25.63			
		Transitional pore	71.47			
	Testing results	Porosity (%)	2.66			
		Displacement pressure (MPa)	2.07			
		Saturation medium pressure (MPa)	45.79			
		Pore medium radius (um)	0.016			
		Maximum mercury saturation (%)	71.92			
		Average pore radius (um)	0.066			
		Mercury drainage efficiency (%)	58.18			
Pore shape	Open pore					
Connectivity	Good					
Pore fractal model	$\lg(1-S_{Hg})=(D-3)\lg P_c+(3-D)\lg P_{min}$ $D=2.59$					
 <p>Nitrogen adsorption/desorption curves of Yuanzhuang coal</p>	Pore distribution (%)	Mesopore	23.54	It is favorable to CBM adsorption, desorption and diffusion.	It is favorable to CBM adsorption, desorption and diffusion.	
		Transitional pore	43.3			
		Micropore	33.16			
	Testing results	Specific surface area (m ² /g)	0.561			
		Pore volume (mL/g)	1.643			
		MPPZ (nm)	4.016			
	Pore shape	Wedge-shaped pore				
Pore fractal model	$\ln(V/V_0) = C + A[\ln(\ln(P_0/P))]$ $D_1=2.18, D_2=2.65$					

Figure 10. Comprehensive analysis of the pore structure based on mercury injection and low-temperature nitrogen experiments from Yuanzhuang coals.

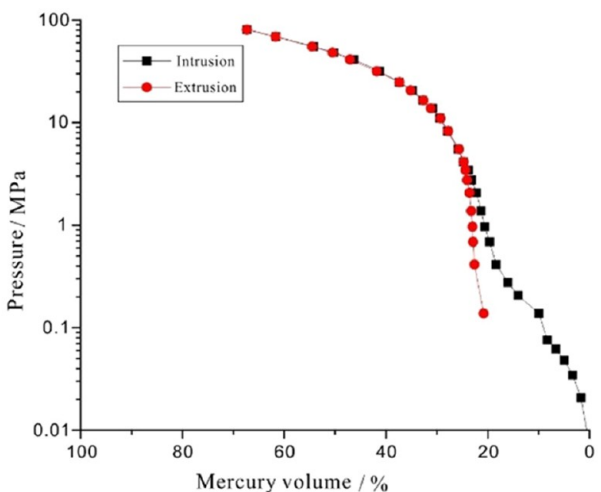
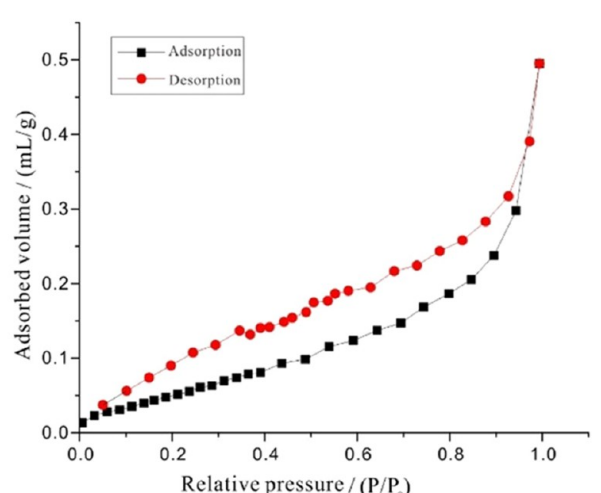
Pore structure testing method	Pore structure parameter	Value	Evaluation	General analysis	
 <p>Mercury injection/extrusion curves of Hengyuan coal</p>	Pore distribution (%)	Macropore	33.32	A poor connectivity, it is unfavorable to CBM diffusion and seepage	It is unfavorable to CBM adsorption, desorption, seepage and CBM production
		Mesopore	13.8		
		Transitional pore	52.87		
	Testing results	Porosity (%)	1.53		
		Displacement pressure (Mpa)	0.14		
		Saturation medium pressure (Mpa)	47.94		
		Pore medium radius (um)	0.016		
		Maximum mercury saturation (%)	67.32		
		Average pore radius (um)	0.839		
		Mercury drainage efficiency (%)	67.09		
Pore shape	Semi-closed pore				
Connectivity	Bad				
Pore fractal model	$\lg(1-S_{Hg}) = (D-3)\lg P_c + (3-D)\lg P_{min}$ $D=2.78$				
 <p>Nitrogen adsorption/desorption curves of Hengyuan coal</p>	Pore distribution (%)	Mesopore	24.17	It is favorable to CBM desorption, unfavorable to adsorption	
		Transitional pore	38.44		
		Micropore	37.39		
	Testing results	Specific surface area (m ² /g)	0.254		
		Pore volume (mL/g)	0.766		
		MPPZ (nm)	4.026		
	Pore shape	Plate pore			
Pore fractal model	$\ln(V/V_0) = C + A[\ln(\ln(P_0/P))]$ $D_1=1.98, D_2=2.68$				

Figure 11. Comprehensive analysis of the pore structure based on mercury injection and low-temperature nitrogen experiments from Hengyuan coals.

the regulation of fixed carbon content significantly influences the adsorption properties of coal, resulting in the transformation of

coal chemical composition and structure by coal metamorphism.¹¹ The Langmuir pressure decreases with increasing

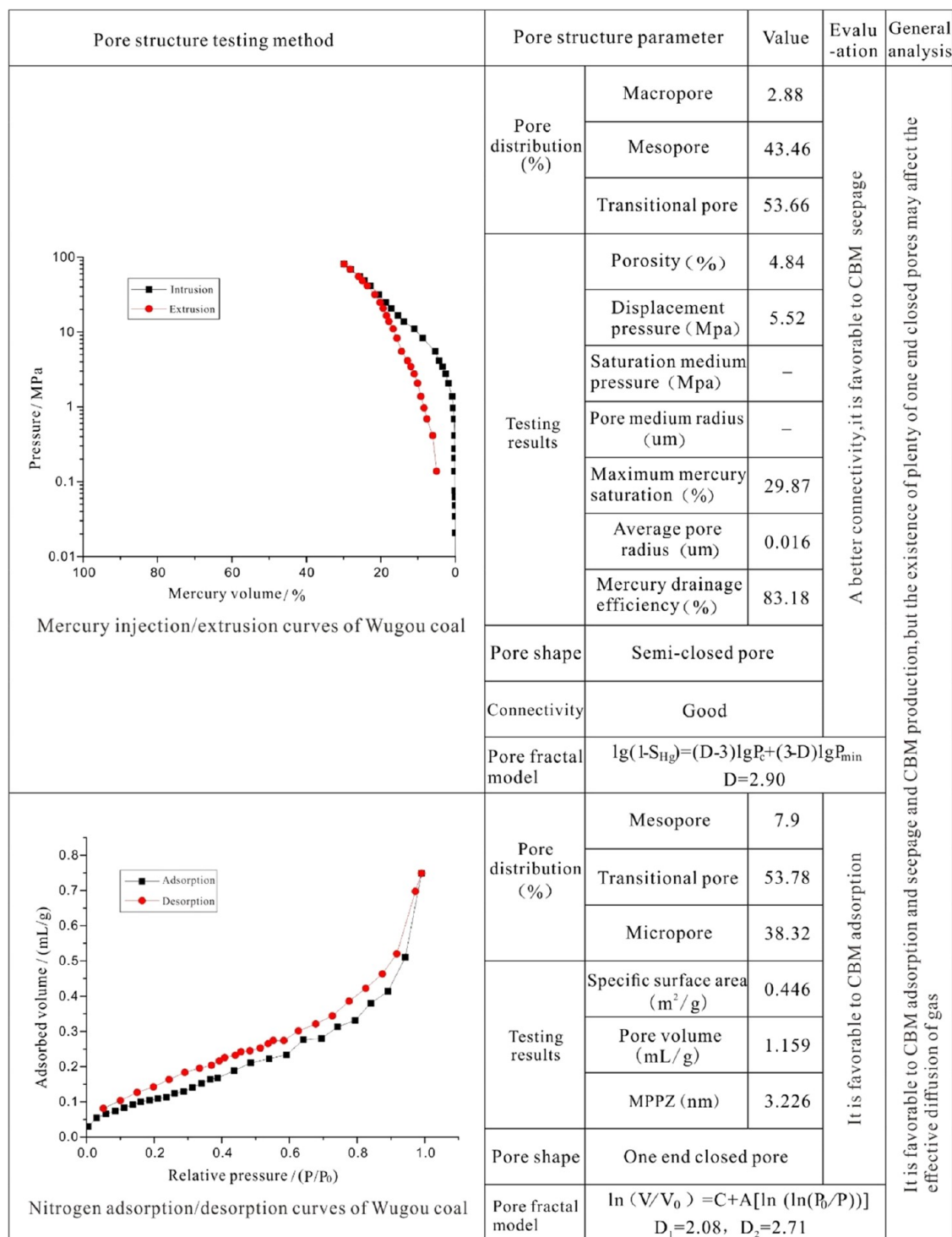


Figure 12. Comprehensive analysis of the pore structure based on mercury injection and low-temperature nitrogen experiments from Wugou coals.

Table 4. Experimental Results of Nuclear Magnetic Resonance of Coal in the Huaibei Coalfield

sampling site	porosity /%	T_2 cutoff values/ms	irreducible fluid saturation/%	movable fluid saturation/%	permeability/mD
Yuanzhuang mine	2.4	25.64	86.57	13.43	0.0031
Hengyuan mine	1.08	0.65	91.2	8.8	0.000049
Guobei mine	2.04	0.32	27.14	72.86	0.49
Haizi mine	0.63	0.4	6.46	93.54	0.13
Wugou mine	2.23	0.31	9.73	90.27	8.31

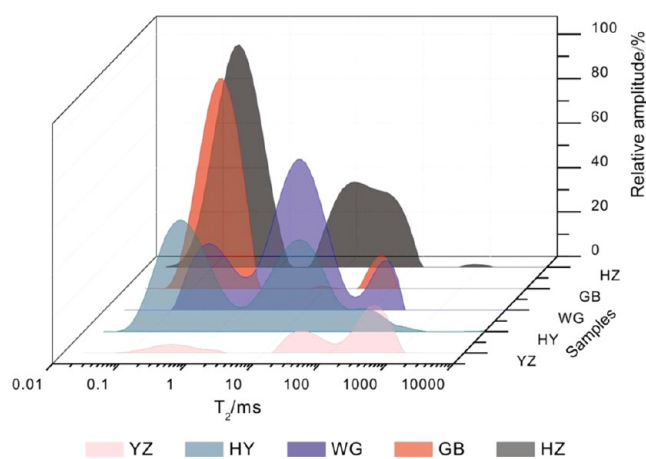


Figure 13. T_2 relaxation time distribution of Huaibei coal samples.

coal rank (Figure 15c), indicating that the CH_4 desorption capacity becomes challenging during the high-pressure stage and easy during the low-pressure stage.

4.5. Coalbed Methane Favorable Area in the Deep Huaibei Coalfield. The selection of CBM favorable areas is a basic prerequisite for its successful exploration and development.⁴² The evaluation methods commonly used at present

include multilevel fuzzy mathematics, gray clustering, weighted average, and comprehensive evaluation.^{43,44} Based on the method of multilevel fuzzy mathematics, the 25 deep gas-bearing evaluation units with burial depths greater than 1500 m can be divided into four mining areas in the Huaibei Coalfield. According to the weight of each evaluation index and the score of each evaluation unit, the evaluation results of the favorable prediction area are obtained based on the complexity of structure, abundance of resources, coal thickness, burial depth, and gas content (Table 5). Specifically, a total score less than 2.5 is considered unfavorable, 2.5–3.5 is considered favorable, and greater than 3.5 is considered favorable. The evaluation results show that the deep Xiaoxi in the Suixiao coal mining, deep Nanping, deep Taoyuan–Qinan, deep Pengqiao, northern Zhuxianzhuang in the Suxian coal mining, deep Renlou–Zhaoji, and Xutuan deep in the Linhuan coal mining are favorable areas for CBM exploration in the Huaibei Coalfield. However, the deep Haizi, deep Qingtuan, deep Yuandian, and deep Suntuan–Yangliu in the Linhuan mining area, Lilou, western Guobo, deep Gucheng, Baliqiao, and deep Xuguanglou in the Guoyang mining area, northern Dangshan, deep Zhangdatun, Wangdazhuang, deep Muji, deep Dayanwu, deep Zhengyaozhuang, and deep Liuxiaomiao in the Suixiao mining area are unfavorable areas for CBM exploration.

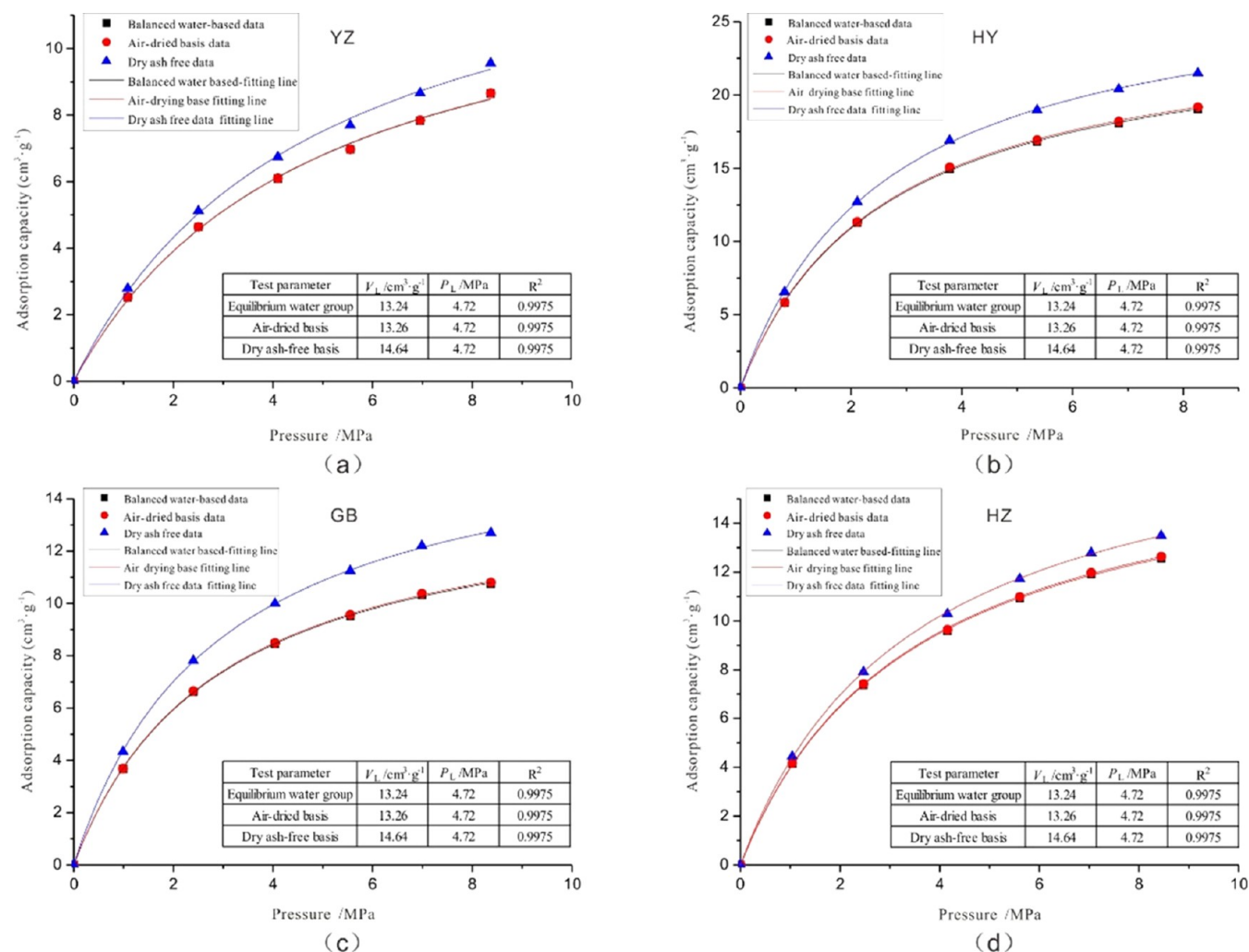


Figure 14. Isothermal adsorption curves of coal samples from the Huaibei Coalfield at 30 °C.

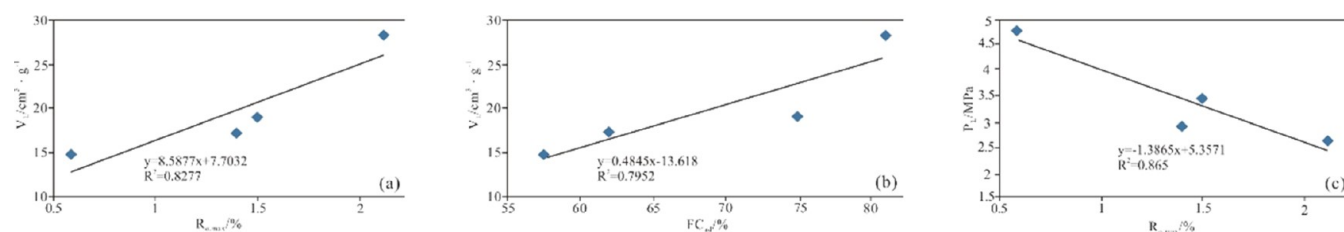


Figure 15. Influence factors of the CH₄ isothermal adsorption experiment from Huaibei coals.

Table 5. Evaluation Results of the Deep CBM Prediction Area in the Huaibei Coalfield^a

evaluation unit		structural complexity	resource abundance (10 ⁸ m ³ /km ²)	coal thickness(m)	burial depth (m)	gas content	comprehensive score	evaluation result
Suixiao coal mining	Northern Dangshan	medium-complex (3)	0.3(1)	3.01(3)	1000–2000(3)	6(5)	1.57	disadvantageous
	Deep Zhangdatun	medium-complex (3)	0.2(1)	3.5(3)	1200–2000(3)	6(5)	1.57	disadvantageous
	Southern Zhangdatun	medium-complex (3)	0.3(1)	4.2(5)	200–1000(2)	4(2)	1.37	disadvantageous
	Wangdazhuang	medium-complex (3)	0.3(1)	2.25(3)	600–1500(8)	10(7)	2.14	disadvantageous
	Deep Xiaoxi	moderate (4)	0.1(2)	2.68(3)	700–2000(7)	12(9)	2.52	relatively favorable
	Deep Muji	complex (1)	0.5(1)	4.45(5)	1000–1500(5)	8(6)	1.74	disadvantageous
	Deep Dayanwu	medium-complex (3)	0.6(2)	4.6(5)	900–1500(6)	10(7)	2.29	disadvantageous
	Deep Zhengyaozhuang	complex (1)	0.1(1)	2.5(3)	1500–2000(2)	8(6)	1.33	disadvantageous
	Liuxiaomiao	medium-complex (3)	0.4(1)	4(5)	200–1900(8)	6(5)	2.12	disadvantageous
Guoyang coal mining	Lilou	medium-complex (3)	0.4(1)	4.5(5)	1100–1900(3)	4(2)	1.44	disadvantageous
	Western Guohao	medium-complex (3)	0.4(1)	4.5(5)	900–2000(4)	7(6)	1.95	disadvantageous
	Deep Guohao	medium-complex (3)	0.4(1)	5.5(5)	500–2000(2)	7(6)	1.81	disadvantageous
	Deep Gucheng	medium-complex (3)	0.3(1)	4.5(5)	1500–2000(2)	6(5)	1.7	disadvantageous
	Baliqiao	medium-complex (3)	0.7(2)	8.57(7)	700–2000(7)	7(6)	2.45	disadvantageous
	Deep Xuguanglou	medium-complex (3)	0.6(2)	8.86(7)	1200–1900(2)	5(3)	1.77	disadvantageous
Linhuai Coal mining	Deep Haizi	medium-complex (3)	0.7(2)	10.2(9)	300–17000(4)	12(9)	2.77	disadvantageous
	Deep Qingtuan	medium-complex (3)	0.9(2)	10.8(9)	1200–2000(3)	8(6)	2.37	disadvantageous
	Deep Yuandian	medium-complex (3)	0.6(2)	8.69(7)	1500–2000(2)	6(5)	1.99	disadvantageous
	Deep Suntuan–Yangliu	medium-complex (3)	0.7(2)	8.0(7)	1000–2000(3)	10(7)	2.28	disadvantageous
	Deep Renlou–Zhaoji	moderate (5)	0.9(2)	15.6(9)	1600–2000(2)	10(7)	2.69	relatively favorable
	Deep Xutuan	moderate (5)	1.1(3)	16.3(9)	1500–2000(2)	6(5)	2.56	relatively favorable
Suxian Coal mining	Deep Nanping	moderate (5)	1.2(4)	11.2(9)	1200–2000(3)	8(6)	2.83	relatively favorable
	Deep Taoyuan–Qinan	moderate (5)	0.6(2)	9.29(9)	1500–1900(2)	14(9)	2.91	relatively favorable
	Pengqiao	moderate (5)	0.6(2)	4.5(7)	700–900(9)	7(6)	2.87	relatively favorable
	Northern Zhuxianzhuang	medium-complex (3)	1.1(3)	9(8)	400–1800(6)	8(6)	2.57	relatively favorable

^aNote: Each parameter is assigned a score in brackets.

5. CONCLUSIONS

- (1) The coal maceral in the Huaibei Coalfield is dominated by vitrinite, with the maximum vitrinite reflectance ranging from 0.7 to 2.5%. The Huaibei coal quality is

characterized by medium-high ash yield, low to very low sulfur content, low phosphorus, and medium-high calorific value.

- (2) The coals with medium rank have the best developed pore-fracture system. From low-ranked coals to medium-ranked coals, the volume of adsorption and seepage pores decreases but the fracture volume increases due to the stronger dehydration and coal matrix shrinkages. From medium-ranked coals to high-ranked coals, adsorption pores have a significant advantage, suggesting a higher CH₄ adsorption capacity.
- (3) There is a positive correlation among fixed carbon content, coal rank, and Langmuir volume, which can be attributed to the transformation of the coal chemical composition and structure by coal metamorphism.
- (4) The evaluation results show that the deep Xiaoxi in the Suixiao coal mining area, deep Nanping, deep Taoyuan–Qinan, deep Pengqiao, northern Zhuxianzhuang in the Suxian coal mining area, deep Renlou–Zhaoji, and Xutuan deep in the Linhuan mining area are favorable areas for CBM exploration in the Huaibei Coalfield.

■ AUTHOR INFORMATION

Corresponding Author

Haihai Hou – College of Mining, Liaoning Technical University, Fuxin 123000, China; orcid.org/0000-0002-9891-979X; Email: houmensihai@163.com

Authors

Xuejiao Zhou – College of Environmental Science and Engineering, Liaoning Technical University, Fuxin 123000, China

Bo Hu – College of Mining, Liaoning Technical University, Fuxin 123000, China

Qian He – College of Mining, Liaoning Technical University, Fuxin 123000, China

Xiangqin Huang – College of Mining, Liaoning Technical University, Fuxin 123000, China

Complete contact information is available at:

<https://pubs.acs.org/10.1021/acsomega.4c00027>

Notes

The authors declare no competing financial interest.

■ ACKNOWLEDGMENTS

The coal sample collection received great assistance from Zhen Li, Sheng Zhao, Xuétian Wang, Benliang Chen, and Dawei Zhang. This study was also supported by the National Natural Science Foundation of China (42102223) and the China Postdoctoral Science Foundation (2021M693844; 2022T150284).

■ REFERENCES

- (1) Hou, H. H.; Shao, L. Y.; Liang, G. D.; Tang, Y.; Li, Y. N.; Zhang, J. Q. *Sedimentary Characteristics and Geological Conditions of Coalbed Methane Accumulation in Xishanyao Formation, Southern Margin of Junggar Basin*; China University of Mining and Technology Press: Xuzhou, 2022.
- (2) Shao, L. Y.; Hou, H. H.; Tang, Y.; Lu, J.; Qiu, H. J.; Wang, X. T.; Zhang, J. Q. Selection of strategic replacement areas for CBM exploration and development in China. *Nat. Gas Ind. B* **2015**, *2* (2–3), 211–221.
- (3) Chen, Y.; Tang, D. Z.; Xu, H.; Li, Y.; Meng, Y. J. Structural controls on coalbed methane accumulation and high production models in the eastern margin of Ordos Basin, China. *J. Nat. Gas Sci. Eng.* **2015**, *23*, 524–537.
- (4) Hou, H. H.; Shao, L. Y.; Tang, Y.; Zhao, S.; Yuan, Y.; Li, Y. N.; Mu, G. Y.; Zhou, Y.; Liang, G. D.; Zhang, J. Q. Quantitative characterization of low-rank coal reservoirs in the southern Junggar Basin, NW China: Implications for pore structure evolution around the first coalification jump. *Mar. Petrol. Geol.* **2020**, *113*, No. 104165.
- (5) Liu, D. M.; Yao, Y. B.; Tang, D. Z.; Tang, S.; Che, Y.; Huang, W. H. Coal reservoir characteristics and coalbed methane resource assessment in Huainan and Huaibei coalfields, Southern North China. *Int. J. Coal Geol.* **2009**, *79* (3), 97–112, DOI: [10.1016/j.coal.2009.05.001](https://doi.org/10.1016/j.coal.2009.05.001).
- (6) Zhang, Q.; Jiang, W. P.; Jiang, Z. B.; Li, B. G.; Du, X. F.; Wu, X. P.; Zhao, J. Z.; Fan, Y.; Fan, Z. Q.; Han, B. S.; Xu, Y. B.; Liu, B. G. Present situation and technical research progress of coalbed methane surface development in coal mining areas of China. *Coal Geol. Explor.* **2023**, *51* (1), 139–158.
- (7) Liu, X. F.; Wang, Z. P.; Song, D. Z.; He, X. Q.; Yang, T. Variations in surface fractal characteristics of coal subjected to liquid CO₂ phase change fracturing. *Int. J. Energy Res.* **2020**, *44* (11), 8740–8753.
- (8) Hou, H. H.; Shao, L. Y.; Tang, Y.; Li, Z.; Zhao, S.; Yao, M. L.; Wang, X. T.; Zhang, J. Q. Pore structure characterization of middle- and high-ranked coal reservoirs in northern China. *AAPG Bull.* **2023**, *107* (2), 213–241.
- (9) Hodot, B. B. *Outburst of Coal and Coalbed Gas (Chinese Translation)*; China Industry Press: Beijing, 1966; pp 27–30.
- (10) Shi, J. Q.; Durucan, S. In *Gas Storage and Flow in Coalbed Reservoirs: Implementation of a Bidisperse Pore Model for Gas Diffusion in a Coal Matrix*, SPE Annual Technical Conference and Exhibition; One Petro, 2005; pp 169–175.
- (11) Hou, H. H.; Shao, L. Y.; Li, Y. H.; Li, Z.; Wang, S.; Zhang, W. L.; Wang, X. T. Influence of coal petrology on methane adsorption capacity of the middle Jurassic coal in the Yuqia Coalfield, northern Qaidam Basin, China. *J. Pet. Sci. Eng.* **2017**, *149*, 218–227.
- (12) Mastalerz, M.; Drobniak, A.; Strapoć, D.; Acost, W. S.; Rupp, J. Variations in pore characteristics in high volatile bituminous coals: Implications for coal bed gas content. *Int. J. Coal Geol.* **2008**, *76* (3), 205–216.
- (13) Mohammad, S. A.; Arumugam, A.; Robinson, R. L., Jr; Gasem, K. High-pressure adsorption of pure gases on coals and activated carbon: measurements and modeling. *Energy Fuels* **2012**, *26* (1), 536–548.
- (14) Yao, Y. B.; Liu, D. M.; Tang, D. Z.; Tang, S. H.; Huang, W. H.; Liu, Z. H.; Che, Y. Fractal characterization of seepage-pores of coals from China: an investigation on permeability of coals. *Comput. Geosci.* **2009**, *35* (6), 1159–1166.
- (15) Guo, R.; Akkutlu, K. M.; Kantzas, A. Laboratory investigation on the permeability of coal during primary and enhanced coalbed methane production. *J. Can. Pet. Technol.* **2007**, *47* (10), 27–32, DOI: [10.2118/08-10-27](https://doi.org/10.2118/08-10-27).
- (16) Mathews, J. P.; Campbell, Q. P.; Xu, H.; Halleck, P. A review of the application of X-ray computed tomography to the study of coal. *Fuel* **2017**, *209*, 10–24.
- (17) Dong, K.; Jia, J. C.; Gong, Z. W.; Wu, Y. Study on pore structure and pressure-sensitive effect of tectonic coal in Huaibei Xutuan mine. *Coal Geol. Explor.* **2019**, *47* (2), 58–65.
- (18) Fang, L. C.; Li, G. H.; Li, D. D.; Li, H. Z.; Liu, J. Analysis on the CBM extraction effect of the horizontal wells in the coal seam roof in Luling coal mine in Huaibei. *Coal Geol. Explor.* **2020**, *48* (6), 155–160.
- (19) Zhao, Z. G.; Xue, S. Multiple-level tectonic control of coalbed methane occurrence in the Huaibei Coalfield of Anhui Province, China. *Energies* **2022**, *15* (14), No. 4977, DOI: [10.3390/en15144977](https://doi.org/10.3390/en15144977).
- (20) Hou, H. H.; Shao, L. Y.; Wang, S.; Xiao, Z. H.; Wang, X. T.; Li, Z.; Mu, G. Y. Influence of depositional environment on coalbed methane accumulation in the Carboniferous–Permian coal of the Qinshui Basin, northern China. *Front. Earth Sci.* **2019**, *13* (3), 535–550.
- (21) Colombera, L.; Shiers, M. N.; Mountney, N. P. Assessment of backwater controls on the architecture of distributary-channel fills in a tide-influenced coastal-plain succession: Campanian Neslen Formation, USA. *J. Sediment. Res.* **2016**, *86* (5), 476–497.
- (22) Xu, H.; Tang, D. Z.; Li, S.; Tao, S. Characteristics of paleo-fluid of coal-bearing strata and its influence on the properties of CBM reservoirs

- in the Western Guizhou Province, China. *Energy Sources, Part A* **2016**, 38 (4), 466–471.
- (23) Ye, J. C.; Tao, S.; Zhao, S. P.; Li, S.; Chen, S. D.; Cui, Y. Characteristics of methane adsorption/desorption heat and energy with respect to coal rank. *J. Nat. Gas Sci. Eng.* **2022**, 99, No. 104445.
- (24) Tao, S.; Pan, Z. J.; Tang, S. L.; Chen, S. D. Current status and geological conditions for the applicability of CBM drilling technologies in China: A review. *Int. J. Coal Geol.* **2019**, 202, 95–108.
- (25) Chen, H. D.; Jiang, J. Y.; Chen, X. J.; Xu, C. T. Differences in coal bed methane occurrence for different regions of igneous erosion in the Haizi coal mine, Huaibei coalfield, China. *J. Nat. Gas Sci. Eng.* **2014**, 21, 732–737.
- (26) Kang, W. B.; Li, W.; Dong, Y. P.; Zhang, L.; Zhao, J. X.; Sheir, F. Multi-stage metamorphism and deformation of the North Qinling Orogenic Belt: Constraints from petrology, geochronology, and structural analysis of the Qinling Complex. *Gondwana Res.* **2022**, 105, 201–216.
- (27) Xu, H.; Tang, D. Z.; Mathews, J. P.; Zhao, J. L.; Li, B. Y.; Tao, S.; Li, S. Evaluation of coal macrolithotypes distribution by geophysical logging data in the Hancheng Block, eastern margin, Ordos Basin, China. *Int. J. Coal Geol.* **2016**, 165, 265–277.
- (28) Tao, S.; Pan, Z. J.; Chen, S. D.; Tang, S. L. Coal seam porosity and fracture heterogeneity of macrolithotypes in the Fanzhuang Block, southern Qinshui Basin, China. *J. Nat. Gas Sci. Eng.* **2019**, 66, 148–158.
- (29) Hou, H. H.; Shao, L. Y.; Liang, G. D.; Tang, Y.; Zhang, H. J.; Zhang, J. Q. Repeated wildfires in the middle Jurassic Xishanyao Formation (Aalenian and Bajocian Ages) in northwestern China. *Acta Geol. Sin. (Engl. Ed.)* **2022**, 96 (5), 1752–1763.
- (30) Hou, H. H.; Shao, L. Y.; Tang, Y.; Li, Y. N.; Liang, G. D.; Xin, Y. L.; Zhang, J. Q. Coal seam correlation in terrestrial basins by sequence stratigraphy and its implication for paleoclimate and paleoenvironment evolution. *J. Earth Sci.* **2023**, 34 (2), 556–570.
- (31) Jian, K.; Fu, X. H.; Ding, Y. M.; Wang, H. D.; Li, T. Characteristics of pores and methane adsorption of low-rank coal in China. *J. Nat. Gas Sci. Eng.* **2015**, 27, 207–218.
- (32) Zhao, Y. X.; Sun, Y. F.; Liu, S. M.; Wang, K.; Jiang, Y. D. Pore structure characterization of coal by NMR cryoporometry. *Fuel* **2017**, 190, 359–369.
- (33) Xin, F. D.; Xu, H.; Tang, D. Z.; Yang, J. S.; Chen, Y. P.; Cao, L. K.; Qu, H. X. Pore structure evolution of low-rank coal in China. *Int. J. Coal Geol.* **2019**, 205, 126–139.
- (34) Ren, J. G.; Song, Z. M.; Li, B.; Liu, J. B.; Lv, R. S.; Liu, G. F. Structure feature and evolution mechanism of pores in different metamorphism and deformation coals. *Fuel* **2021**, 283, No. 119292.
- (35) Cai, Y. D.; Liu, D. M.; Liu, Z. H.; Zhou, Y. F.; Che, Y. Evolution of pore structure, submaceral composition and produced gases of two Chinese coals during thermal treatment. *Fuel Process. Technol.* **2017**, 156, 298–309.
- (36) Su, X. B.; Zhang, L. P.; Lin, X. Y. Influence of coal rank on coal adsorption capacity. *Nat. Gas Ind.* **2005**, 25 (1), 19–21.
- (37) Zhang, W. J.; Ju, Y. W.; Wei, M. M.; Wang, G. C. Study on characteristics and mechanism of adsorption/desorption on different metamorphic-deformed coal reservoirs. *Earth Sci. Front.* **2015**, 22 (2), 232–242.
- (38) Yee, D.; Seidle, J. P.; Hanson, W. B. Gas Sorption on Coal and Measurement of Gas Content. In *Hydrocarbon from Coal*; Law, B. E.; Rice, D. D., Eds.; AAPG Studies in Geology, 1993; pp 203–218.
- (39) Sun, F. R.; Liu, D. M.; Cai, Y. D.; Qiu, Y. K. Coal rank-pressure coupling control mechanism on gas adsorption/desorption in coalbed methane reservoirs. *Energy* **2023**, 270, No. 126849.
- (40) Zhao, X. L.; Tang, D. Z.; Xu, H.; Tao, S.; Chen, Z. L. Effect of coal metamorphic process on pore system of coal reservoirs. *J. China Coal Soc.* **2010**, 35 (9), 1506–1511.
- (41) Zhang, S.; Zhang, C.; Zhang, M.; Liu, X.; Xue, S. Model construction and optimization of coal molecular structure. *J. Mol. Struct.* **2023**, 1290, No. 135960.
- (42) Sun, B.; Shao, Y. W.; Gao, Z. H.; Li, J. A.; Sun, B. L.; Yang, M. F.; Zhou, J. M.; Yao, H. P.; Sun, F. J.; Shao, L. Y. Coalbed methane enrichment characteristics and exploration target selection in the Zhuozishan Coalfield of the western Ordos Basin, China. *ACS Omega* **2022**, 7 (48), 43531–43547.
- (43) Chen, F. J.; Jiang, X. M.; Wu, C. F.; Zhou, H.; Gao, B.; Zhang, S. S. Evaluation of coalbed methane resources in Xinjing Baoan block based on PCA, TOPSIS, & MLFM. *Energy Explor. Exploit.* **2022**, 40 (5), 1457–1481.
- (44) Liang, H. B.; Sun, Y. Q.; Li, G. L.; Li, Z. L. Gray relational clustering model for intelligent guided monitoring horizontal wells. *Neural Comput. Appl.* **2019**, 31 (5), 1339–1351.